Online-Journals.org

iJOE International Journal of Online and Biomedical Engineering

iJOE | eISSN: 2626-8493 | Vol. 19 No. 14 (2023) | OPEN ACCESS

https://doi.org/10.3991/ijoe.v19i14.42725

PAPER

Discriminative Approach Lung Diseases and COVID-19 from Chest X-Ray Images Using Convolutional Neural Networks: A Promising Approach for Accurate Diagnosis

Hicham Benradi(✉), Issam Bouganssa, Ahmed Chater, Abdelali Lasfar

High School of Technology Salé, Mohammadia School of Engineering, Systems Analysis, Information Processing, and Industrial Management Laboratory, Mohammed V University, Rabat, Morocco

benradi.hicham@gmail.com

ABSTRACT

Medical imaging treatment is one of the best-known computer science disciplines. It can be used to detect the presence of several diseases such as skin cancer and brain tumors, and since the arrival of the coronavirus (COVID-19), this technique has been used to alleviate the heavy burden placed on all health institutions and personnel, given the high rate of spread of this virus in the population. One of the problems encountered in diagnosing people suspected of having contracted COVID-19 is the difficulty of distinguishing symptoms due to this virus from those of other diseases such as influenza, as they are similar. This paper proposes a new approach to distinguishing between lung diseases and COVID-19 by analyzing chest x-ray images using a convolutional neural network (CNN) architecture. To achieve this, pre-processing was carried out on the dataset using histogram equalization, and then we trained two sub-datasets from the dataset using the Train et Test, the first to be used in the training phase and the second to be used in the model validation phase. Then a CNN architecture composed of several convolution layers and fully connected layers was deployed to train our model. Finally, we evaluated our model using two different metrics: the confusion matrix and the receiver operating characteristic. The simulation results recorded are satisfactory, with an accuracy rate of 96.27%.

KEYWORDS

COVID-19, histogram normalization, convolutional neural network (CNN), confusion matrix, ROC curve

1 INTRODUCTION

The arrival of COVID-19 has changed the lives of people in every country in the world. The danger of this pandemic is distinguished by its speed of propagation and the damage that it can cause, especially to the elderly or chronically ill patients,

Benradi, H., Bouganssa, I., Chater, A., Lasfar, A. (2023). Discriminative Approach Lung Diseases and COVID-19 from Chest X-Ray Images Using Convolutional Neural Networks: A Promising Approach for Accurate Diagnosis. *International Journal of Online and Biomedical Engineering (iJOE)*, 19(14), pp. 131–141. https://doi.org/10.3991/ijoe.v19i14.42725

Article submitted 2023-06-30. Revision uploaded 2023-08-02. Final acceptance 2023-08-02.

something that has pushed researchers from all fields to try to find a solution to stop it. Among the solutions that have been made available to health personnel is the chest x-ray, because the virus attacks primarily the lungs and causes respiratory problems that can cause death.

The field of medical imaging has been revolutionized by the integration of adapted image processing techniques from the field of computer vision [1] [2] [3] [4] [5]. Among these techniques, the use of convolutional neural networks (CNNs) is widely used in the field of deep learning. CNNs are known for extracting features and performing classifications, making them a robust approach. They consist of multiple layers, including convolution, pooling, density, and flattening layers, each with its own distinct function. The objective of these architectures is to train the machine to detect the presence of diseases in various types of medical images, such as x-rays, chest radiographs (CXRs), computerized tomography (CT) scans, magnetic resonance imaging (MRI) scans, and so forth. CNNs are used in many fields, including robotics [6], facial expressions [7], education [8] [9], and also in the medical field such as the detection of brain tumors [10] [11] [12], prostate cancer [13] [14], lung nodules [15], COVID-19 [16] [17], and breast cancer [18] [19].

We have developed a deep learning model based on a CNN architecture using a database of chest x-rays called COVID-QU, and we intend to present it in this paper. The aim of the study was to distinguish three cases: COVID-positive patients, those with a viral lung infection, and those considered normal. To achieve this, we preprocessed all the images in the database using the histogram equalization technique. This method resulted in a balanced distribution of intensities, improving the ability to assess measurement similarity. Next, we divided the dataset into two distinct subsets: the training set and the test set. Finally, we implemented our CNN architecture to obtain an efficient model for classifying chest x-rays into one of the three categories mentioned above. The overall aim of our study was to help healthcare professionals rapidly assess patients' conditions and reduce the time needed for diagnosis.

2 RELATED WORKS

Several research studies have been carried out to train a model based on CNN architecture to determine or confirm the presence of COVID-19 in a chest x-ray. The authors of the article [20] proposed a new CovidXrayNet model based on the EfficientNet-B0 architecture. The simulation results reached an accuracy of 95.82%. Another method was developed in [21] aimed at detecting COVID-19-infected pneumonia from chest x-ray images based on the DAC scheme by applying two pre-processing steps to the used dataset to eliminate the majority of the diaphragm region, then a CNN architecture based on transfer learning is used to classify the chest x-ray into three classes (COVID-infected pneumonia, COVID-uninfected pneumonia, and normal case). The simulation results of this method, called CNN-based computer-aided design (CAD), recorded an accuracy value of 95%. Another method based on a hybrid structure containing a BiLSTM bidirectional long-term memory layer was implemented in [22] and recorded an accuracy value of 98.70%. In addition, in a paper [23], an approach combining a CNN architecture and a long-term memory (LTM) network was used to perform an automatic diagnosis of COVID-19 from CXR images. Simulation results demonstrated an accuracy of

up to 99.4%. The authors in [24] used the transfer learning technique using image augmentation to train and validate several pre-trained deep CNN architectures. The best results were recorded using the DENSENet201 architecture, with an accuracy value of 99.70%.

3 METHODOLOGY

3.1 Method

Our model was trained using the COVID-QU database of chest x-ray images [25] [26]. This database comprises a total of 15,153 images, divided into three categories: COVID-19 positive, normal, and viral pneumonia. By way of illustration, here are a few examples of images from this database, as shown in Figure 1.

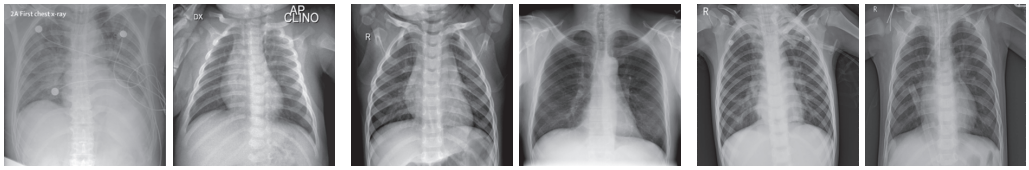

(a) (b) (c)

Fig. 1. Overview of some images from the dataset used, showing: (a) COVID-19 positive cases, (b) normal cases, and (c) viral pneumonia cases

All the images in the database are divided into three categories: 1345 images for the viral pneumonia case, 3616 images for the COVID-19 case, and 10192 images for the normal cases, as illustrated in the form of a graph in Figure 2.

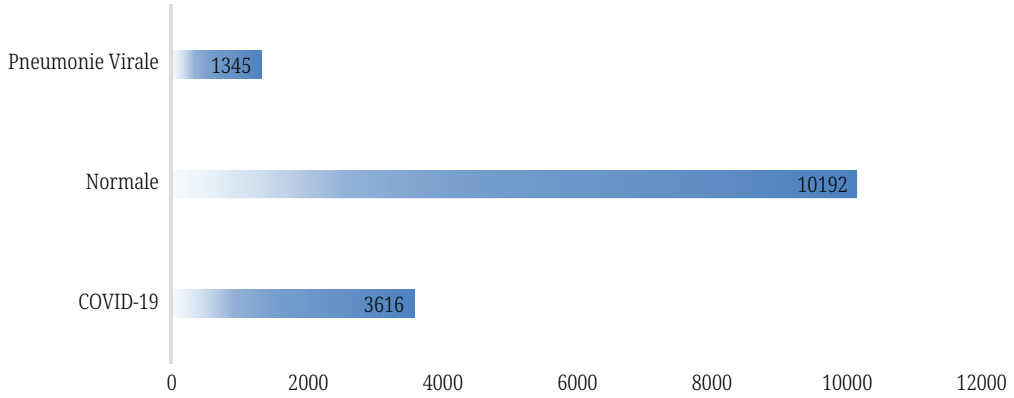

Fig. 2. Distribution of all the images in the database by category

The analysis of the used data set of the three categories using the graphs below (Figure 3), which represent the graphical distribution of the maximum, minimum, and average pixel values about the density of the images, shows that the average pixel value for the negative COVID cases is higher than 0.014 and lower than 0.016. The average pixel value for the positive COVID cases is greater than 0.004 and less than 0.006. In normal cases, the average pixel value is greater than 0.002 and less than 0.006.

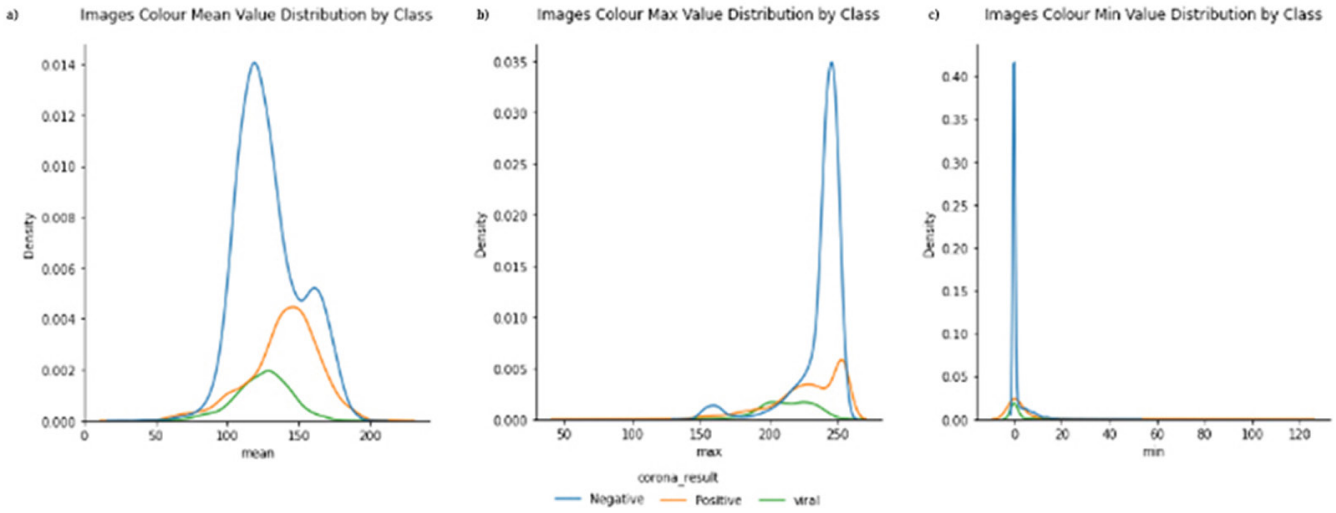

Fig. 3. Categorical distributions of values about density, (a) mean values, (b) maximum value, and (c) minimum values

Our approach is based on the use of a convolutional neural network architecture to develop a model capable of distinguishing three cases: normal, viral lung infection, and COVID-19. The details of how we achieved this goal are substantiated in this section.

Our process began with an initial pre-processing phase, during which we prepared the images to be used. During this stage, we assigned appropriate labels to each image according to their category (COVID or normal). Next, we applied histogram equalization to modify the contrast of each image and distribute intensities over the entire range of values. In this way, we created new images by independently manipulating each pixel of the original image using its cumulative histogram.

Histogram equalization, introduced in [19] by Gonzalez and Woods, involves applying a transform T to each pixel of an image coded with L levels. To do this, we calculated the number of occurrences of a level x_k, denoted NK. The probability of the occurrence of a pixel of level x_k in an image is represented by equation (1).

$$p_x(x_k) = p(x = x_k) = \frac{n_k}{n}, 0 \le k < L \tag{1}$$

Where: n represents the number of pixels in an image and p_x denotes the histogram normalized to a scale of [0, 1].

For each pixel of value x_k, a new value SK = $T(x_k)$ is associated with the transformation T. The definition of this transformation is given by equation (2).

$$T(x_k) = (L-1)\sum_{j=0}^{k} p_x(x_j) \tag{2}$$

Where: $\sum_{j=0}^{k} p_x(x_j)$ = the cumulative histogram.

Figure 4 below shows an example of this operation applied to a chest x-ray.

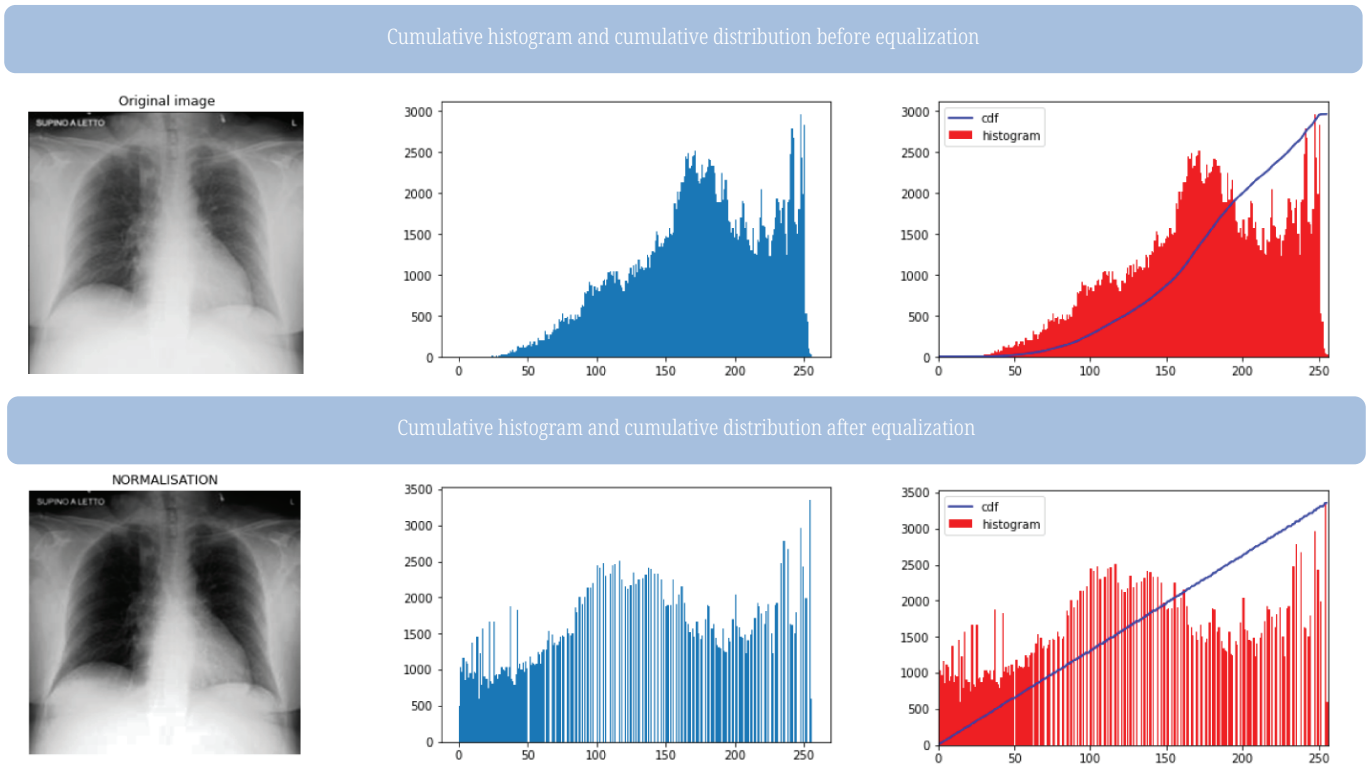

Fig. 4. The application of histogram equalization on a chest x-ray image

After performing histogram equalization operation, we observed a uniform redistribution of intensity across the entire image. This is demonstrated in Figure 4 through the cumulative histogram analysis. This operation adjusted the contrast of each pixel independently, distributing intensity values over the entire available range. In this way, dark regions have been lightened and light regions have been darkened, improving the visibility of details in the image. The structural similarity index (SSIM) is also calculated to ensure image quality after the histogram equalization operation. In all cases, the SSIM score is always greater than 0.7, indicating good structural similarity between the original image and the equalized image after histogram equalization.

Once the pre-processing of the dataset is complete, we proceed with its preparation. This preparation aims to unify the size of the images (64 × 64) and also to label all images by their corresponding class. We then create two datasets: train and test. The first, train, comprises 80% of the dataset and will be used in the training phase of our model. The remaining 20% of the test dataset will be used to validate our model. Next, a CNN architecture was developed to create our model. This architecture is defined as follows:

Three successive convolution layers using different filters (32, 64, and 128) with a kernel of size 3 × 3 and the RELU activation function.

- Three Maxpool layers with a value of (2, 2), which halves the size of the input.
- A flattening layer is used to transform all values into a one-dimensional vector.
- Two fully connected layers: the first uses the RELU activation function, followed by a dropout layer set at 0.5 to avoid overfitting, and the second uses the Softmax activation function for classification.

Figure 5 provides an overview of the proposed method.

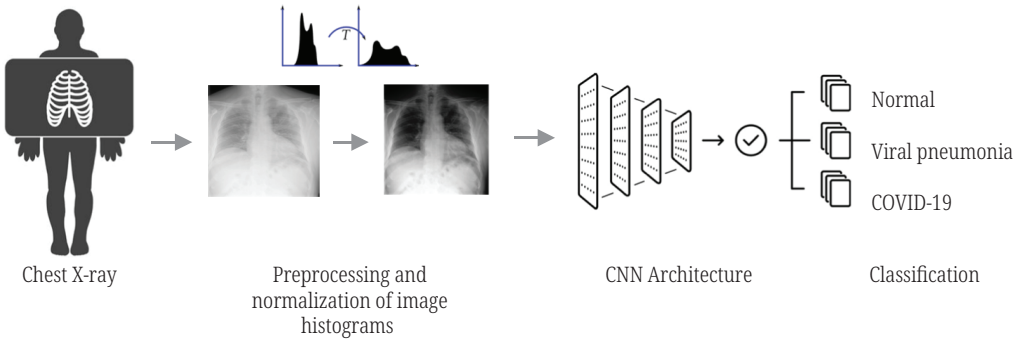

Fig. 5. Using CNN architecture

Once our model had been trained, we proceeded to evaluate it using various metrics such as accuracy, specificity, precision, sensitivity, F1_score, and receiver operating characteristic (ROC), calculated using equations (5, 6, 8, 9, and 10).

Performance is assessed using the confusion matrix, a table showing actual and predicted values. This matrix is used to evaluate the model using several metrics, including:

$$Accuracy = \frac{TP + TN}{TP + TN + FP + FN} \tag{5}$$

$$Recall = \frac{TP}{TP + FN} \tag{6}$$

$$precision = \frac{TP}{TP + FP} \tag{7}$$

$$F1\_score = \frac{precision \times Sensitivity}{precision + Sensitivity} \tag{8}$$

Where, *TF* represent true negative, *TP* represent true positive, *FN* represent false negative, and *FP* represent false positive.

The ROC curve is a method used to evaluate the performance of a binary classifier. It consists of a graphical representation linking the rate of true positives to the rate of false positives. This curve is used to analyze the sensitivity (ability to detect true positives) and specificity (ability to avoid false positives) of the classifier at different classification thresholds. By examining the ROC curve, we can evaluate the classifier's overall performance and choose the optimum threshold according to the specific needs of the problem.

3.2 Results

The results of our experiments were obtained using the COVID-QU image database, with the aim of evaluating similarity metrics and comparing the impact of each operation performed on the set of images. Our model was trained for 100 epochs, using a recall function to prevent overfitting of weights. All the results of our experiments are listed in Table 1.

Table 1. Results of simulations

	Precision	Recall	F1-Score	Support
Normal	97.81%	96.85%	97.33%	2036
Viral pneumonia	96.99%	93.14%	95.02%	277
COVID	91.85%	95.82%	93.79%	718
Accuracy		96.27%		3031
Macro avg	95.55%	95.27%	95.38%	3031
Weighted avg	96.33%	96.27%	96.28%	3031

We note that the proposed method recorded results exceeding 91% on all evaluation metrics.

The confusion matrix (Figure 6), generated from the test part, consists of 3031 images distributed over the three categories, of which 2036 belong to the normal category, 277 to the viral pneumonia category, and 718 to the COVID category. The exploitation of the confusion matrix generated gave remarkable results. The model was able to classify 657 images in the right category among the 718 used for the test in the case of the COVID category and recorded an accuracy value of 91.85%.

For the normal category, the model was able to classify 1992 images in the right category among 2036 and missed just 44 images classifying them in the other two categories of which 16 were classified as belonging to the viral pneumonia category and 28 images were classified as belonging to the COVID category. For this category, the accuracy reached a value of 97.81%. For the viral pneumonia category, the model using 277 images for the test was able to classify 269 images in the appropriate class, but it missed only eight images, classifying six in the normal category and two in the COVID category.

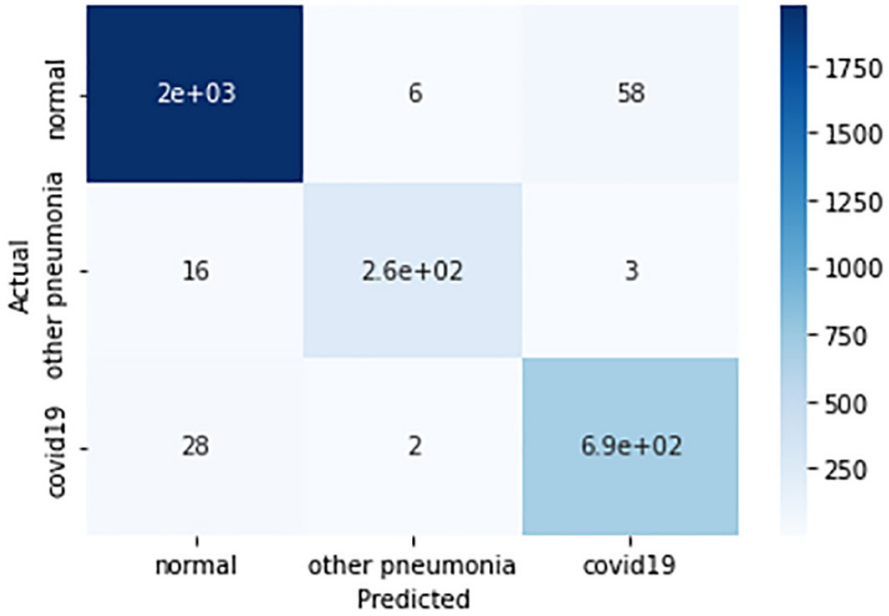

Fig. 6. Confusion matrix

Figure 7 shows the evaluation of similarity scores using the ROC curve. This curve was used to evaluate the categorical model and demonstrate the effectiveness of the proposed method in terms of similarity scores. The results obtained indicate satisfactory performance, confirming the method's ability to discriminate between different categories with precision.

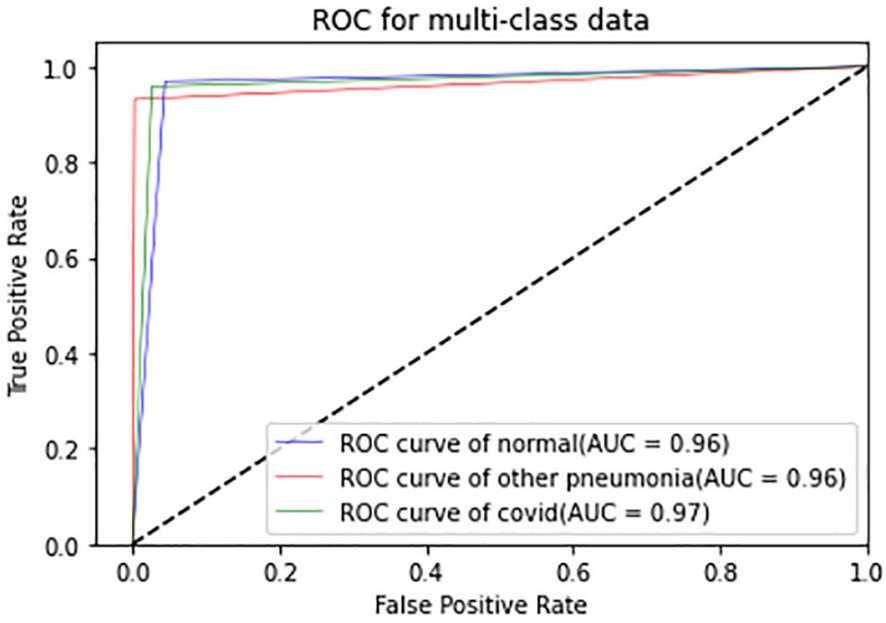

Fig. 7. Graphical representation of the ROC curves of each category

3.3 Discussion

To better evaluate the results obtained by the proposed method compared with the results of related works. Table 2 gathers all these results. Our proposed method recorded satisfactory results on all metrics (accuracy, specificity, precision, sensitivity, and F1_score) compared to other works.

Table 2. Comparative tables of results of related work

	Accu	Precision	Recall	F1 Score
COVIDXRAYNET [10]	95.82	96.93	95.43	96.16
CNN-based CAD [11]	95	88	95	94
mAlexNet + BiLSTM [12]	98.7	98.77	98.76	98.76
CNN-LSTM [13]	99.4	99.56	99.1	99.13
DENSENet201 [14]	99.7	99.7	99.7	99.7
Proposed Method	**96.27**	**96.33**	**96.27**	**96.28**

The graphical representation in Figure 8 shows that the results of our proposed method are competitive and have outperformed some results of other works.

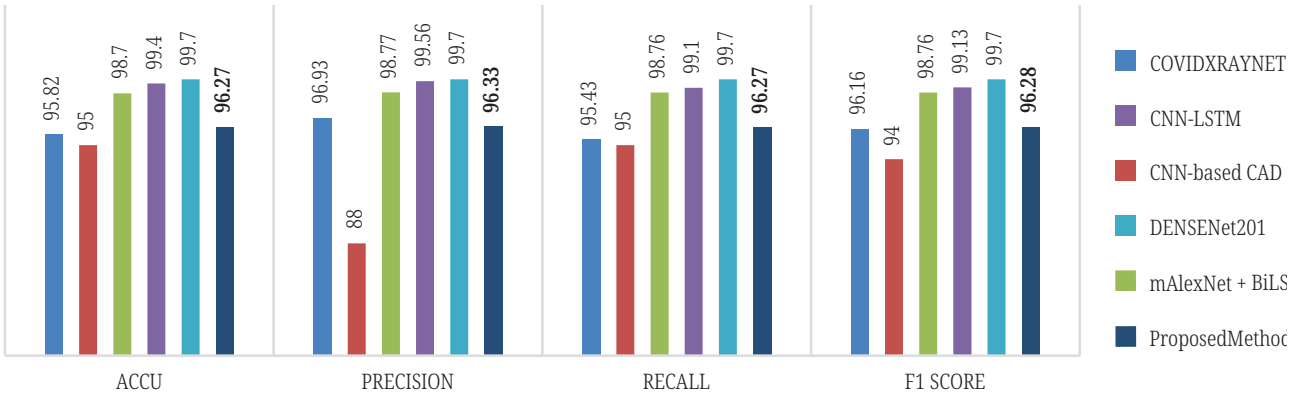

Fig. 8. Graphical representation of the results of the related work and the proposed method results

4 CONCLUSION

In this article, a new approach has been implemented to differentiate lung disease and COVID-19 disease from chest x-ray images. The approach consists of applying processing to all the images used, using the histogram equalization technique to obtain an intensity distribution over the whole of each image. These processed images are then used as input data in a CNN architecture to train a model capable of detecting the presence of lung disease and classifying it as either COVID-19 or viral pneumonia. The model evaluation was based on two measures: the confusion matrix and the ROC curve. The results obtained by our method were satisfactory, with an accuracy rate of 96.27%. This accuracy is competitive with results obtained in similar studies. To further improve model performance, it would be advisable to train the database of chest x-ray images and explore other techniques, such as segmentation, to improve similarity scores.

5 REFERENCES

[1] A. Chater and A. Lasfar, "Comparison of robust methods for extracting descriptors and facial matching," in *International Conference on Wireless Technologies, Embedded and Intelligent Systems (WITS)*, Fez, Morocco: IEEE, 2019, pp. 1–4. https://doi.org/10.1109/WITS.2019.8723858

[2] A. Chater, H. Benradi, and A. Lasfar, "Method of optimization of the fundamental matrix by technique speeded up robust features application of different stress images," *International Journal of Electrical and Computer Engineering (IJECE)*, vol. 12, no. 2, p. 1429, 2022. https://doi.org/10.11591/ijece.v12i2.pp1429-1436

[3] B. Hicham, C. Ahmed, and L. Abdelali, "Face recognition method combining SVM machine learning and scale invariant feature transform," *E3S Web Conf.*, vol. 351, p. 01033, 2022. https://doi.org/10.1051/e3sconf/202235101033

[4] H. Benradi, A. Chater, and A. Lasfar, "A hybrid approach for face recognition using a convolutional neural network combined with feature extraction techniques," *International Journal of Artificial Intelligence (IJ-AI)*, vol. 12, no. 2, p. 627, 2023. https://doi.org/10.11591/ijai.v12.i2.pp627-640

[5] Mohammed Jawad Al_Dujaili, H. TH. S. ALRikabi, Nisreen Khalil Abed, and Ibtihal Razaq Niama ALRubeei, "Gender recognition of human from face images using multi-class support vector machine (SVM) classifiers," *Int. J. Interact. Mob. Technol.*, vol. 17, no. 08, pp. 113–134, 2023. https://doi.org/10.3991/ijim.v17i08.39163

[6] T. Ganokratanaa and M. Ketcham, "An intelligent autonomous document mobile delivery robot using deep learning," *Int. J. Interact. Mob. Technol.*, vol. 16, no. 21, pp. 4–22, 2022. https://doi.org/10.3991/ijim.v16i21.32071

[7] H. Echoukairi, M. El Ghmary, S. Ziani, and A. Ouacha, "Improved methods for automatic facial expression recognition," *Int. J. Interact. Mob. Technol.*, vol. 17, no. 06, pp. 33–44, 2023. https://doi.org/10.3991/ijim.v17i06.37031

[8] S. Wen, "An analysis of emotional responses of students in bilingual classes and adjustment strategies," *Int. J. Emerg. Technol. Learn.*, vol. 18, no. 01, pp. 100–114, 2023. https://doi.org/10.3991/ijet.v18i01.37125

[9] M. Niu, "Classification of learning sentiments of college students based on topic discussion texts of online learning platforms," *Int. J. Emerg. Technol. Learn.*, vol. 17, no. 24, pp. 42–56, 2022. https://doi.org/10.3991/ijet.v17i24.35951

[10] M. O. Khairandish, M. Sharma, V. Jain, J. M. Chatterjee, and N. Z. Jhanjhi, "A hybrid CNN-SVM threshold segmentation approach for tumor detection and classification of MRI brain images," *IRBM*, vol. 43, no. 4, pp. 290–299, 2022. https://doi.org/10.1016/j.irbm.2021.06.003

[11] S. M. Mangj, P. H. Hussan, and W. M. R. Shakir, "Efficient deep learning approach for detection of brain tumor disease," *Int. J. Onl. Eng.*, vol. 19, no. 06, pp. 66–80, 2023. https://doi.org/10.3991/ijoe.v19i06.40277

[12] P. Sj and H. N. Prakash, "A features fusion approach for neonatal and pediatrics brain tumor image analysis using genetic and deep learning techniques," *Int. J. Onl. Eng.*, vol. 17, no. 11, p. 124, 2021. https://doi.org/10.3991/ijoe.v17i11.25193

[13] A. Saha, M. Hosseinzadeh, and H. Huisman, "End-to-end prostate cancer detection in bpMRI via 3D CNNs: Effects of attention mechanisms, clinical priori and decoupled false positive reduction," *Medical Image Analysis*, vol. 73, p. 102155, 2021. https://doi.org/10.1016/j.media.2021.102155

[14] L. Duran-Lopez *et al.*, "Wide & Deep neural network model for patch aggregation in CNN-based prostate cancer detection systems," *Computers in Biology and Medicine*, vol. 136, p. 104743, 2021. https://doi.org/10.1016/j.compbiomed.2021.104743

[15] Y. Su, D. Li, and X. Chen, "Lung nodule detection based on faster R-CNN framework," *Computer Methods and Programs in Biomedicine*, vol. 200, p. 105866, 2021. https://doi.org/10.1016/j.cmpb.2020.105866

[16] H. Kumarasinghe, S. Kolonne, C. Fernando, and D. Meedeniya, "U-Net based chest X-ray segmentation with ensemble classification for Covid-19 and pneumonia," *Int. J. Onl. Eng.*, vol. 18, no. 07, pp. 161–175, 2022. https://doi.org/10.3991/ijoe.v18i07.30807

[17] L. R. Ali, S. A. Jebur, M. M. Jahefer, and B. N. Shaker, "Employing transfer learning for diagnosing COVID-19 disease," *Int. J. Onl. Eng.*, vol. 18, no. 15, pp. 31–42, 2022. https://doi.org/10.3991/ijoe.v18i15.35761

[18] C. B. Gonçalves, J. R. Souza, and H. Fernandes, "CNN architecture optimization using bio-inspired algorithms for breast cancer detection in infrared images," *Computers in Biology and Medicine*, vol. 142, p. 105205, 2022. https://doi.org/10.1016/j.compbiomed.2021.105205

[19] M. Desai and M. Shah, "An anatomization on breast cancer detection and diagnosis employing multi-layer perceptron neural network (MLP) and Convolutional neural network (CNN)," *Clinical eHealth*, vol. 4, pp. 1–11, 2021. https://doi.org/10.1016/j.ceh.2020.11.002

[20] M. M. A. Monshi, J. Poon, V. Chung, and F. M. Monshi, "CovidXrayNet: Optimizing data augmentation and CNN hyperparameters for improved COVID-19 detection from CXR," *Computers in Biology and Medicine*, vol. 133, p. 104375, 2021. https://doi.org/10.1016/j.compbiomed.2021.104375

[21] M. Heidari, S. Mirniaharikandehei, A. Z. Khuzani, G. Danala, Y. Qiu, and B. Zheng, "Improving the performance of CNN to predict the likelihood of COVID-19 using chest X-ray images with preprocessing algorithms," *International Journal of Medical Informatics*, vol. 144, p. 104284, 2020. https://doi.org/10.1016/j.ijmedinf.2020.104284

[22] M. F. Aslan, M. F. Unlersen, K. Sabanci, and A. Durdu, "CNN-based transfer learning–BiLSTM network: A novel approach for COVID-19 infection detection," *Applied Soft Computing*, vol. 98, p. 106912, 2021. https://doi.org/10.1016/j.asoc.2020.106912

[23] Md. Z. Islam, Md. M. Islam, and A. Asraf, "A combined deep CNN-LSTM network for the detection of novel coronavirus (COVID-19) using X-ray images," *Informatics in Medicine Unlocked*, vol. 20, p. 100412, 2020. https://doi.org/10.1016/j.imu.2020.100412

[24] M. E. H. Chowdhury *et al.*, "Can AI help in screening viral and COVID-19 pneumonia?" *IEEE Access*, vol. 8, pp. 132665–132676, 2020. https://doi.org/10.1109/ACCESS.2020.3010287

[25] G. Jia, H.-K. Lam, and Y. Xu, "Classification of COVID-19 chest X-Ray and CT images using a type of dynamic CNN modification method," *Computers in Biology and Medicine*, vol. 134, p. 104425, 2021. https://doi.org/10.1016/j.compbiomed.2021.104425

[26] S. Thakur and A. Kumar, "X-ray and CT-scan-based automated detection and classification of covid-19 using convolutional neural networks (CNN)," *Biomedical Signal Processing and Control*, vol. 69, p. 102920, 2021. https://doi.org/10.1016/j.bspc.2021.102920

6 AUTHORS

Hicham Benradi holds a Master's degree in data engineering and software development from the Faculty of Science at Mohamed V University. He is a Ph.D student at the Mohammadia engineering school in Rabat. His research focuses on facial recognition methods and image processing (E-mail: benradi.hicham@gmail.com).

Issam Bouganssa, holds a Bachelor of Science and Technology in mechatronics at the Faculty of Sciences Rabat, specialized Master's degree in microelectronics at the Faculty of Sciences Kenitra, and a PhD student in science and technology for engineers specializing in automation and embedded systems at the LASTIMI Laboratory, Mohammed-V University of Rabat since 2018. He is active in the field of research, embedded systems and industrial computing. He has been a Professor at Mohammed V University in Rabat since 2019, and is a permanent member of the German Physical Society since 2015 (E-mail: issam.bouganssa@gmail.com).

Ahmed Chater holds a Degree in Engineering Sciences and Techniques, specialty: Image Processing, Laboratory of Systems Analysis, Information Processing and Industrial Management, Mohamed V University Rabat (Mohammadia School). His research interest includes the Segmentation and restoration of different types of color and grayscale images, classification and recognition of facial expressions, and machine learning (E-mail: ahmedchater11@gmail.com).

Abdelali Lasfar is a Professor of Higher Education at Mohammed V Agdal University, Salé Higher School of Technology, Morocco. His research focuses on compression methods, indexing by image content and image indexing, and knowledge extraction from images (E-mail: ali.lasfar@gmail.com).